

Neurophotonics

Neurophotonics.SPIEDigitalLibrary.org

Imaging membrane potential changes from dendritic spines using computer-generated holography

Dimitrii Tanese
Ju-Yun Weng
Valeria Zampini
Vincent De Sars
Marco Canepari
Balazs Rozsa
Valentina Emiliani
Dejan Zecevic

Imaging membrane potential changes from dendritic spines using computer-generated holography

Dimitrii Tanese,^{a,†} Ju-Yun Weng,^{b,†} Valeria Zampini,^a Vincent De Sars,^a Marco Canepari,^{c,d,e} Balazs Rozsa,^f Valentina Emiliani,^a and Dejan Zecevic^{b,*}

^aParis Descartes University, Neurophotonics Laboratory, CNRS UMR8250, Paris, France

^bYale University School of Medicine, Department of Cellular and Molecular Physiology, New Haven, Connecticut, United States

^cUniversité Grenoble Alpes and CNRS, Laboratory for Interdisciplinary Physics, UMR 5588, Saint Martin d'Hères, France

^dLaboratories of Excellence, Ion Channel Science and Therapeutics, France

^eInstitut National de la Santé et Recherche Médicale, Grenoble, France

^fInstitute of Experimental Medicine of the Hungarian Academy of Sciences, Budapest, Hungary

Abstract. Electrical properties of neuronal processes are extraordinarily complex, dynamic, and, in the general case, impossible to predict in the absence of detailed measurements. To obtain such a measurement one would, ideally, like to be able to monitor electrical subthreshold events as they travel from synapses on distal dendrites and summate at particular locations to initiate action potentials. It is now possible to carry out these measurements at the scale of individual dendritic spines using voltage imaging. In these measurements, the voltage-sensitive probes can be thought of as transmembrane voltmeters with a linear scale, which directly monitor electrical signals. Grinvald et al. were important early contributors to the methodology of voltage imaging, and they pioneered some of its significant results. We combined voltage imaging and glutamate uncaging using computer-generated holography. The results demonstrated that patterned illumination, by reducing the surface area of illuminated membrane, reduces photodynamic damage. Additionally, region-specific illumination practically eliminated the contamination of optical signals from individual spines by the scattered light from the parent dendrite. Finally, patterned illumination allowed one-photon uncaging of glutamate on multiple spines to be carried out in parallel with voltage imaging from the parent dendrite and neighboring spines. © 2017 Society of Photo-Optical Instrumentation Engineers (SPIE) [DOI: 10.1117/1.NPh.4.3.031211]

Keywords: voltage imaging; holography; dendritic spines; glutamate uncaging.

Paper 17013SSR received Feb. 28, 2017; accepted for publication Apr. 24, 2017; published online May 12, 2017.

1 Introduction

Understanding the biophysical properties and functional organization of single neurons is fundamental to understanding how the brain works. Because the primary function of any nerve cell is to process electrical signals [i.e., membrane potential (V_m) transients], there is a need for detailed spatiotemporal analysis of electrical events in thin axonal and dendritic processes. This requirement resulted in the development of measurement techniques that allow monitoring of the electrical activity of different parts of the same cell simultaneously. A major experimental advance in this field, which also underscored the importance of such measurements, was achieved by the development of the multiple patch-electrode recording method that made possible simultaneous monitoring of V_m transients from two or more dendritic locations on a single neuron.^{1–3} The patch-electrode technique, however, is still limited in its capacity for assessing spatiotemporal patterns of signal initiation and propagation in complex dendritic and axonal processes. Moreover, many subcellular structures, including small diameter terminal dendritic branches as well as dendritic spines and most axon terminals and axon collaterals, are not accessible to electrodes. To overcome these limitations, it was highly desirable to complement the patch-electrode approach with technologies that permit

extensive parallel recordings from all parts of a neuron with adequate spatial and temporal resolution. An adequate temporal resolution in recording neuronal action potential (AP) and synaptic potential signals is in the submillisecond range, as determined by the duration of different phases of the AP and SP waveforms. An adequate spatial resolution is on the order of 1 μm , as determined by the dimensions of neuronal terminal processes and dendritic spines. This spatiotemporal resolution can now be realized using optical recording of V_m changes with organic voltage-sensitive dyes (voltage imaging). The sensitivity of this measurement technique has recently reached a level that permits single-trial optical recordings of AP transients from all parts of a neuron, including axon terminals and collaterals, terminal dendritic branches, and individual dendritic spines. In large part, these developments are based on pioneering work of Grinvald et al. We report here an advance in the capabilities of voltage-sensitive dye recording technology using patterned illumination based on computer-generated holography (CGH) with spatial light modulators (SLM).⁴

1.1 Foundation of Optical Recording of Membrane Potential Transients from Individual Nerve Cells

The feasibility of multiple site optical recording from subregions of individual nerve cells was initially demonstrated using

*Address all correspondence to: Dejan Zecevic, E-mail: dejan.zecevic@yale.edu

[†]These authors contributed equally to this work.

monolayer neuronal culture and extracellular application of the voltage-sensitive dye. Grinvald et al.⁵ showed that voltage-sensitive dyes and multisite optical measurements can be employed successfully to determine conduction velocity, space constants, and regional variations in the electrical properties of neuronal processes in measurements from dissociated neurons in monolayer culture. Both absorption and fluorescence measurements were used in these experiments, and the individual dissociated neurons in a culture dish were stained from the extracellular side by bath application of the dye.⁶ It has also been possible, using the same approach, to study synaptic interactions among several interconnected neurons in culture^{7,8} and the cell-to-cell propagation of the AP in patterned growth cardiac myocytes forming two-dimensional (2-D) hearts in culture.⁹ The monolayer neuronal culture is a low opacity system especially convenient for extracellular staining of the outside cellular membrane. However, primary cultures are networks of neurons that grow under artificial conditions. Therefore, a number of important questions in cellular neurophysiology can only be studied in intact or semi-intact preparations. However, extending the same approach to *in situ* conditions has proven difficult and has been slow to develop. In *in situ* conditions, the extracellular application of fluorescent dyes cannot provide subcellular resolution because of the large background fluorescence from the dye bound indiscriminately to all membranes in the preparation.¹⁰

Based on these arguments, Grinvald et al. designed an approach to optical analysis of electrical events in processes of individual nerve cells. The key conceptual advance was the idea to stain particular neurons *in situ* selectively by intracellular application of an impermeant fluorescent voltage-sensitive dye. This approach was based on pioneering measurements in Larry Cohen's and Brian Salzberg's laboratories at the Marine Biological Laboratory in Woods Hole, performed on the giant axon of the squid, which demonstrated that optical signals may be obtained when the dye is applied from the inside.¹¹⁻¹⁴ In these experiments, optical signals were obtained from the large membrane surface area of the giant axon. Substantial additional efforts were required to demonstrate that the same approach is feasible at the spatial scale of average size neurons and their processes. The initial experiments in this direction, using intracellular labeling with voltage-sensitive dyes, were carried out by Obaid et al.¹⁵ and by Grinvald et al.¹⁶ on leech neurons. The results demonstrated the essential advantages of using intracellular application of fluorescent potentiometric probes. Fluorescence measurements are more effective than absorption measurements when measuring from a small membrane area,¹⁷ particularly in situations where the image of the object (e.g., thin process) is much smaller than the size of the photodetector picture element (pixel).^{18,19} When transmitted light is used, only a small fraction of the total light captured by individual pixels will be modulated by the signal from the neuronal process (dendrite or axon) projected onto that pixel (ΔI). Most of the light will be projected directly and will only contribute to the resting light intensity (I). Thus, the fractional signal ($\Delta I/I$) will be very small. On the other hand, in fluorescence measurements, practically all of the light captured by individual pixels will come from the object (if autofluorescence is negligible) regardless of the fraction of the pixel surface area covered by the image of the object. In now classical experiments on leech neurons,¹⁶ fluorescence measurements were used to record APs and synaptic potential signals from processes

of selectively stained single neurons. As predicted, the S/N was substantially improved relative to prior absorption measurements, but the sensitivity was still too low to be of practical value—the available S/N was insufficient for multiple site optical recording of complex electrical interactions at the level of thin neuronal processes. The limits to the sensitivity of these measurements were determined primarily by (a) the relatively low voltage sensitivity of the available dyes (amino-phenyl styryl dyes, e.g., RH437 and RH461; fractional change in fluorescence intensity per AP, in intracellular application, of the order of 0.01% to 0.1%); (b) the choice of the excitation light bandwidth; and (c) the relatively low intensity of the incident light that could be obtained from a 100-W mercury arc lamp. Despite low sensitivity, these experiments clearly showed the advantages of selective staining of individual neurons by intracellular application of the dye and paved the way for further improvements in sensitivity. At the time, the reported sensitivity was the result of a modest screening effort, suggesting that better signals might be obtained by (a) synthesizing and screening new molecules for higher sensitivity, (b) increasing the concentration of the dye to increase the fluorescence intensity, (c) using an excitation light source capable of providing higher light intensity and better stability, and (d) using detector devices with lower dark-noise and adequate spatial and temporal resolution. Following this rationale, the first substantial improvement in the S/N was obtained by finding an intracellular voltage-sensitive dye with sensitivity in intracellular application two-orders of magnitude higher than what was previously available. The amino-naphthalene styryl dye JPW1114 synthesized by Wuskell and Loew at the University of Connecticut Health Center had the sensitivity expressed as $\Delta F/F$ per AP, in intracellular application, of the order of 10%.²⁰ The higher sensitivity of this dye translates directly into higher S/N .

The second significant improvement in sensitivity was the introduction of cooled, backilluminated CCD cameras. The CCD camera, because it is cooled and can have about 1000 times smaller pixel surface area and proportionally smaller dark currents compared to available diode arrays, exhibits substantially lower dark noise. Following the introduction of CCD cameras, a number of studies demonstrated that the V_m -imaging is quite efficient at the spatial scale of dendritic branches.²⁰⁻²² The available S/N , however, was still not adequate to allow multisite recordings from thin axons and axon collaterals at high frame rates (5 to 10 kHz) without extensive averaging (>100 trials). In addition, it was still not possible to monitor V_m signals at the higher optical magnification and finer spatial scale necessary for resolving electrical events at the level of individual dendritic spines. Clearly, further improvements in sensitivity (expressed as the S/N) were needed.

One way to increase the S/N with a given voltage-sensitive dye is to increase the photon flux (Φ) by increasing the excitation light intensity. Another possibility is to increase the fractional fluorescence change per unit change in V_m (sensitivity of the dye) by choosing the optimal excitation wavelength. Following this rationale, Holthoff et al. used one of the most sensitive voltage-sensitive dyes in terms of S/N (JPW3028^{21,23,24}) and improved both the excitation (and, hence, emission) light intensity and the relative fluorescence change in response to V_m change by utilizing a laser as an illumination source in wide-field epifluorescence microscopy mode.²⁰ In measurements from layer 5 pyramidal neurons in rat visual cortex slices, the light from a frequency-doubled

200-mW diode-pumped Nd:YVO₄ continuous wave laser emitting at 532 nm was directed to a quartz optical fiber coupled to the microscope via a single-port epifluorescence condenser (TILL Photonics) designed to overfill the back aperture of the objective. In this way, approximately uniform illumination of the object plane was attained. In the initial series of experiments with this apparatus, the extent of propagation and the time course of backpropagating action potentials (bAPs) signals were monitored from dendrites at relatively low magnification [the full CCD frame (80 × 80 pixels) corresponded to a 300 × 300 μm area in the object plane]. In this configuration, bAPs could be monitored with unprecedented sensitivity in single-trial measurements at all dendritic sites, including the terminal apical tuft as well as the oblique and the basal dendrites.²⁰ The combined effect of an increase in light intensity and the use of a near-optimal excitation wavelength was a dramatic improvement in the sensitivity of voltage imaging by a factor of about 50 in recording from different sites on neuronal processes.

1.1.1 Voltage imaging from dendritic spines

The high sensitivity of recording from dendrites and axons at relatively low-optical magnification indicated that it should be possible to increase the optical magnification by a factor of 10 and monitor V_m -transients from individual dendritic spines. Recording electrical events from individual dendritic spines is important for several reasons. Spines play a critical role in the input–output transform carried out by an individual neuron. They receive most of the excitatory synaptic inputs in many brain regions and serve as calcium compartments, which appear to be necessary for input-specific synaptic plasticity.^{25–27} In the last decade, a number of investigators (e.g., Winfried Denk, Rafael Yuste, Karel Svoboda, Bernardo Sabatini, and Haruo Kasai) revisited previously well-articulated theoretical questions and ideas^{28,29} and analyzed open problems in spine physiology with the aid of innovative experimental technologies. The methodology has been developed to measure Ca²⁺ signals from individual spines with great precision using two-photon microscopy, and many aspects of spine physiology related to Ca²⁺ signaling have been illuminated.³⁰

The electrical behavior of spines, however, is less well understood and controversial. For a long time, the electrical role of spines had to be considered on purely theoretical grounds because it was technically impossible to measure V_m -signals from individual spines. Theoretical work^{28,31,32} and, more recently, several experimental studies^{27,33–39} speculated or provided indirect evidence that the electrical characteristics of dendritic spines might have important implications for integrative function and for the plastic properties of neurons. Other studies based on diffusion measurements^{40,41} as well as on multicompartmental modeling^{29,41} indicated that spines may not play a significant electrical role. This question was unresolved because it has never been possible to directly document the electrical behavior of dendritic spines owing to the limited sensitivity of the available measurement techniques at the requisite spatial resolution. Thus, a critical challenge, both conceptually and technically, was to develop an approach for the direct analysis of V_m signals from individual dendritic spines. The improvement in sensitivity described above made this type of recording possible.²⁰ In these measurements, a magnified image of a spiny dendrite of a stained neuron was projected onto a CCD camera and fluorescence intensity changes were monitored from

multiple locations. The bAP-related signals from dendritic spines were clearly resolved in single-trial measurements and the S/N was further improved by averaging a small number (4 to 9) of trials. In these wide-field fluorescence measurements, it was documented that the interference from scattered light was insignificant in the superficial layers of the slice.²⁰ This study showed by direct measurement that bAP signals from spines and dendrites did not differ significantly.

1.1.2 Further improvements in sensitivity

On the conceptual level, a key open question regarding the electrical role of dendritic spines is whether the hypothetical electrical isolation of synapses on spine heads caused by a narrow spine neck provides specific functions that are not available to synapses on dendrites. Several such functions with wide implications have been proposed based on computational modeling and indirect evidence: (1) spines reduce location-dependent variability of local EPSPs and, thus, standardize and enhance synaptic activation of both NMDA channels and voltage-gated channels; (2) changes in structure and electrical resistance of the spine neck under activity control mediate the induction of synaptic plasticity underlying learning and memory formation; (3) electrical properties of spines promote either linear or non-linear (depending on evidence) dendritic integration and associated forms of plasticity, thus fundamentally enhancing the computational capabilities of neurons; (4) spines have the capacity to act as discrete electrogenic compartments that amplify synaptic potentials by activation of voltage-sensitive channels. These functions, if directly demonstrated, would define the electrical role of spines. However, a direct demonstration of the electrical behavior of dendritic spines would require recording of unitary subthreshold synaptic responses at the spatial scale of individual spines with adequate sensitivity and temporal resolution to allow quantitative analysis. The best existing sensitivity that allowed optical monitoring of bAP from dendritic spines^{20,42} was insufficient because EPSP signals would be 5- to 10-fold smaller in amplitude. Thus, a substantial improvement in the sensitivity of optical recording was required to allow measurements of unitary EPSP signals from individual spines. This was recently accomplished by (a) a further increase in the excitation intensity from a laser at the wavelength that has the best signal and (b) minimizing photodynamic damage by restricting the excitation light to a small area (18 μm × 18 μm) around the spine of interest and by briefly lowering oxygen concentration in the extracellular solution during optical recording.^{43,44} This technology was utilized to monitor the electrical transients in the spine head and the parent dendrite at the base of the spine. The results showed that synapses on these spines are not electrically isolated by the spine neck to a significant extent.⁴³ From these measurements, we concluded that the success rate (limited by light scattering and by the extent of photodynamic damage) was too low to allow studies of more complex electrical phenomena in dendritic spines. We recently showed how one-photon CGH illumination improved voltage imaging of APs on adjacent axons and dendrites.⁴⁵ Additionally, CGH can allow multisite uncaging under one-^{46,47} and two-photon^{48–50} excitations. Here, we apply CGH to generate both imaging and photostimulation patterns and improve several aspects of the voltage imaging investigation of dendritic spines.

2 Methods

2.1 Slices, Patch-Clamp Recording and Intracellular Application of Dyes

All procedures were performed in accordance with Public Health Service Policy on Humane Care and Use of Laboratory Animals and approved by Yale University Institutional Animal Care, as well as by Paris Descartes Ethics Committee for Animal Research (registered number CEEA34.EV.118.12) in accordance with European Union institutional guidelines. The experiments were carried out on somatosensory cortex slices from 15- to 21-day-old rats of either sex. The rats were decapitated following deep halothane anesthesia, the brain was quickly removed, and 300- μm -thick coronal cortical slices were cut in ice-cold solution. Slices were incubated at 37°C for about 30 min and then maintained at room temperature (23°C to 25°C). The standard extracellular solution used during recording contained (in mM): 125 NaCl, 25 NaHCO₃, 20 glucose, 2.5 KCl, 1.25 NaH₂PO₄, 2 CaCl₂, and 1 MgCl₂, pH 7.4 when bubbled with a 5% CO₂ gas mixture balanced with 95% O₂. Somatic whole-cell recordings in current clamp or voltage-clamp mode were made with 4 to 6 M Ω patch pipettes using a Multiclamp 700B amplifier (Axon Instruments Inc., Union City, California). Voltage-clamp recordings were made with series resistance compensation set at 70%. The pipette solution contained (in mM): 120 K-gluconate, 3 KCl, 7 NaCl, 4 Mg-ATP, 0.3 Na-GTP, 20 HEPES, and 14 tris-phosphocreatin (pH 7.3, adjusted with KOH) and 0.8 mM of the voltage-sensitive dye JPW3028.⁴³ In all experiments, an attempt was made to identify layer 5 pyramidal cells with intact dendrites in one plane of focus close to the surface of the slice (to minimize light scattering) using infrared differential interference contrast (DIC) video microscopy. The recordings were carried out from spines on superficial basal dendrites at different distances from the soma (range 30 to 120 μm). Labeling of pyramidal neurons with the voltage-sensitive dye was carried out by free diffusion from a somatic patch electrode in the whole-cell configuration. We used the most successful voltage probe for intracellular application, JPW3028, a close analog of JPW1114^{20,45,51} with similar voltage sensitivity available from Thermo Fisher Scientific as D6923. The electrode tips were first filled with dye-free solution by applying negative pressure and then back filled with the solution containing the voltage probe (0.8 mM). The patch electrode was detached from the neuron by forming an outside-out patch after staining was accomplished, as determined by measuring resting fluorescence intensity from the soma. Following the staining period, the preparation was incubated for an additional 1.5 to 2 h at room temperature to allow the voltage-sensitive dye to spread into dendritic processes and spines. Before optical recording, the cell was repatched to obtain electrical recording using an electrode filled with dye-free intracellular solution.

2.2 Optical Setup

The recording setup was built around a stationary upright microscope (Olympus BX51; Olympus Inc.) equipped with a high-spatial resolution CCD camera for infrared DIC video microscopy and for detailed morphological reconstruction of dye-loaded neurons (Photometrics, CoolSnap ES2) and a fast data acquisition camera with relatively low-spatial resolution (80 \times 80 pixels) and exceptionally low read noise (NeuroCCD-

SM, RedShirtImaging LLC, Decatur, Georgia) used for voltage imaging.

The microscope was coupled with two holographic-patterned illumination paths, one for voltage imaging and one for uncaging. The simplified schematic of the setup is shown in Fig. 1(a). The voltage imaging part was based on a 532-nm diode-pumped laser source (MLL-FN-532-450-5-LAB-TTL, Changchun New Industries Optoelectronics Tech. Co. Ltd., Changchun, China). The laser beam was attenuated by neutral density filters, enlarged by a telescope, and cleaned by a 50- μm pinhole before it was directed to the sensitive area of a liquid crystal of an SLM (Hamamatsu X10468-01). The reflected beam was projected onto the back focal plane of 100 \times microscope objective (NA = 1.0 water dipping, Olympus) by an afocal telescope formed by L1 (f = 500 mm) and L2 (f = 250 mm) and a dichroic mirror D1 (FF560-FDi01-25x36, Semrock). The zero-order nonmodulated components reflected from the SLM were suppressed by an intermediate point block. A defocus of the beam was explicitly introduced before the SLM such that the zero-order focus was displaced by around 5 cm. For the diffracted first-order component, the defocus was compensated with a spherical Fresnel lens at the SLM. In this way, the point block for the zero-order component did not significantly perturb the propagation of the holographic pattern.⁴⁵ For voltage imaging, the illumination power delivered to the slice depended on several factors, including the level of voltage-sensitive dye staining, the depth of the dendritic branch with spines, and the exact pattern of stimulation. Thus, the illumination power delivered to the preparation varied in the range of 0.05 to 0.6 mW.

The uncaging illumination was obtained using a commercial module for holographic light patterning (Phasor-3i Intelligent Imaging Innovation, Inc. Denver, Colorado), modulating a 405-nm laser source (Obis Coherent, 100 mW) controlled by LaserStack and SlideBook software (3i Intelligent Imaging Innovation). The illumination power delivered to each uncaging spot varied between 0.1 to 0.5 mW. The imaging and uncaging beam were combined using a dichroic mirror D2 (Di03-R405/488/561/635-25x36, Semrock). The induced fluorescence from a voltage-sensitive probe was long-pass filtered LPF (FF01-593/LP-25, Semrock) and imaged using NeuroCCD-SM camera.

2.3 Computer-Generated Holography

Multipoint CGH patterns for both imaging and uncaging were generated using a modified weighted Gerchberg and Saxton algorithm (GS).^{47,52} The relative intensity between spots was controlled by adjusting their weight in the input pattern of the algorithm.^{53,54} The pattern and the corresponding wGS-generated phase profiles were defined, computed, and addressed to the SLM using “Wavefront Designer IV,” in house software written in C++ with Qt 4.4.0 and fftw 3.1.2. Calibration and characterization of the generated patterns were performed by detecting induced fluorescence on a thin film of rhodamine 6G spin-coated on a coverslip. The multipoint patterns shown on Fig. 1(b) acquired on the NeuroCCD camera were used to calibrate the exact positioning of the holographic spots. By introducing a correcting stretch, translation, and rotation transformation to the input pattern that was provided to the algorithm, we could achieve submicrometric precision in spot positioning. The experimentally recorded beam size [Fig. 1(b)] results from the convolution of excitation (405 or 532 nm) and the detection point spread function (PSF) at the wavelength of the collected

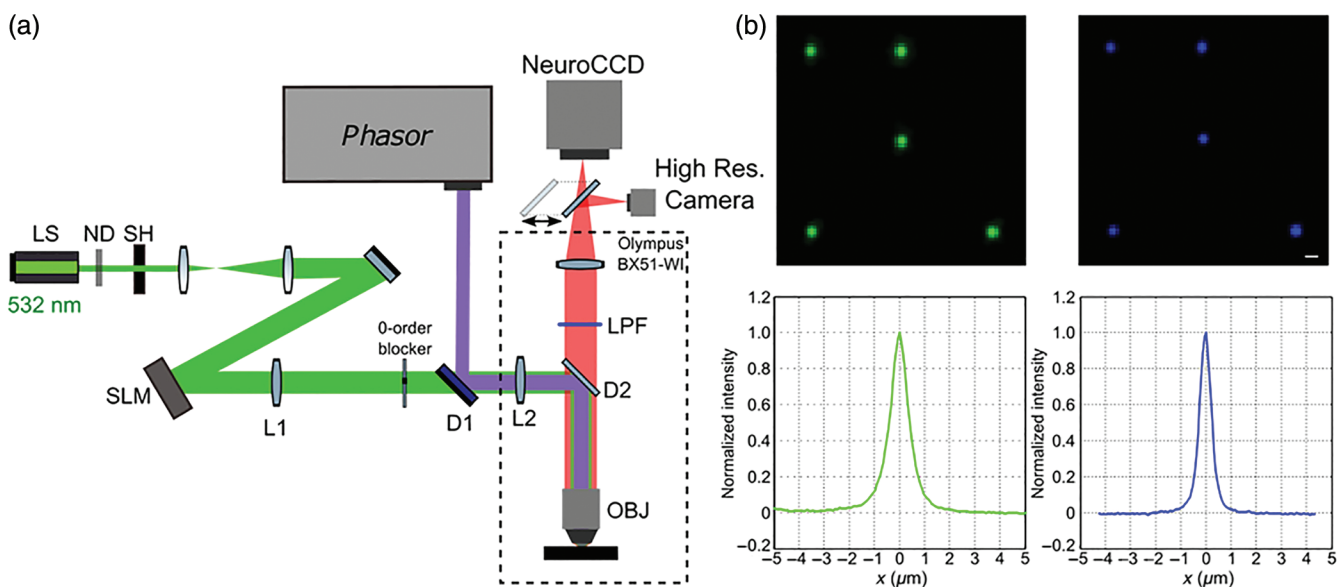


Fig. 1 Two-color CGH illumination: (a) diagram of the optical setup for holographic illumination patterns at 532 and 405 nm. The 532-nm (green) laser beam from a solid-state laser is attenuated by neutral density filters (ND), enlarged by a telescope, and directed to the liquid crystal SLM. The plane of the SLM is projected with an afocal telescope (L1 and L2) to the back aperture of a microscope objective (OBJ). The 405-nm patterned beam (violet) is generated by a commercial module (phasor) and coupled to the 532-nm beam path through a dichroic mirror D1. The patterned beams are reflected toward the objective by the dichroic mirror D2. The collected fluorescence is filtered by the long pass filter (LPF) and directed either to the high-resolution camera or to the high-speed NeuroCCD camera using a movable mirror. (b) Upper panels: Fluorescence pattern generated by a 532-nm (right) and 405-nm (left) digital holography on a thin layer of rhodamine 6G as detected with the NeuroCCD. These patterns were used to calibrate the submicrometric positioning of the holographic spots. Scale bar 1 μm . Lower panels: spatial profile of the rhodamine emission generated by a 532-nm (green) or 405-nm (blue) CGH spot recorded with the high-resolution camera.

rhodamine emission (filtered by the LPF filter). We estimated the effective excitation beam size based on the nominal value of the detection PSF and the measured experimental profile [acquired by high-resolution camera and shown in Fig. 3(b)] to be $\sim 0.3 \mu\text{m}$ (FWHM) for the 405-nm spots and $\sim 0.7 \mu\text{m}$ for the 532-nm ones. A slight under-filling of the objective back aperture was used to increase the size of holographic spots of the 532-nm imaging pattern to better match the size of a typical spine. A similar GS algorithm^{54,55} was also applied to generate a large 532-nm holographic spot (diameter $\sim 25 \mu\text{m}$) that was used to mimic wide-field illumination. The large illumination spot was used to obtain an image of dye-loaded dendrites and identify structures of interest on the NeuroCCD for voltage imaging. Because extended holographic shapes are characterized by randomly distributed intensity inhomogeneities (speckles), wide-field images (as shown in Fig. 3) were obtained by averaging five different speckle patterns. The obtained wide-field fluorescence images of selected dendritic segments were used to define the pattern of holographic illumination for both imaging and uncaging (Fig. 3). We adjusted different illumination intensities for different illumination spots to enhance signals from specific regions of interest. Typically, the spots covering spine heads were adjusted to have 2 to 10 times stronger illumination intensities relative to those on the dendritic shaft. For voltage imaging, laser light was gated by a high-speed shutter (Uniblitz LS6, driver D880C) for 10- to 30-ms recording trails. Recordings were carried out at a frame rate of 2 or 5 kHz. Acquisition and analysis of data were carried out with NeuroPlex software (RedShirtImaging). For glutamate uncaging, we used

bath-applied DNI-glutamate (5 mM) provided by Femtonics KFT (Budapest, Hungary). Illumination pattern for uncaging consisted of single or multiple spots placed near individual spine heads, approximately at a distance of $0.5 \mu\text{m}$. The actual spatial relationship between the uncaging spots and spine heads was uncertain at the submicrometer spatial scale because of light scattering in the brain tissue. Short pulses (0.2 to 0.3 ms) of patterned illumination were applied to induce local glutamate release near spine heads.

2.4 Data Analysis

Subthreshold EPSP signals and bAP signals were recorded typically for 30 ms at a frame rate of 2 or 5 kHz at room temperature kept at 25°C to 27°C or at near physiological temperature of 32°C to 34°C . Repetition of typically nine trials was acquired and averaged. Analysis and display of data were carried out using the NeuroPlex software (RedShirtImaging) written in IDL (Exelis Visual Information Solutions, Boulder, Colorado) and custom visual basic routines. No correction for background fluorescence was carried out because it was found to be negligible under holographic illumination restricted to several spots on labeled dendrites. The signal alignment software was used to correct for temporal jitter in AP initiation, as well as for possible small movements of the preparation during averaging.⁴³ In the temporal domain, AP signals were aligned by cross-correlation of the electrically recorded APs in each trial to the reference signal acquired at the start of averaging. In the spatial domain, camera images were aligned in 2-D offline by image cross-

correlation to compensate for possible small lateral movements of the preparation. Correct focus of the image in the z -dimension was verified frequently; small adjustments were often necessary. The spatially and temporally aligned signals were averaged and slow changes in light intensity due to bleaching of the dye were corrected by dividing the data by an appropriate dual exponential function derived from the recording trials with no stimulation. Dual exponential fitting requires an algorithm for least-squares estimation of nonlinear parameters. We used the Levenberg–Marquardt algorithm. Subthreshold optical signals were calibrated on an absolute scale (in mV) by normalizing to an optical signal from a bAP, which has a known declining amplitude along basal dendrites, as it has been determined by patch-pipette recordings.^{56,57} In an earlier study,⁴³ we experimentally confirmed the previously reported result⁵⁸ showing that this method of calibration produces the same results as normalizing signals to optical recordings corresponding to long hyperpolarizing pulses delivered to the soma that attenuate relatively little as they propagate along dendrites.

3 Results

We integrated a voltage-imaging setup with a system for two independent patterned illumination systems based on CGH, implemented with the use of two SLM systems (see Sec. 2). Our goal was to improve several aspects of voltage imaging of subthreshold synaptic potentials from individual dendritic spines evoked by glutamate uncaging. We focused on the limitations in accuracy and sensitivity of optical recording of membrane potential signals imposed by light scattering and by photodynamic damage. We also carried out experiments to confirm the functionality of patterned illumination in voltage imaging combined with simultaneous illumination patterns for multisite glutamate uncaging.

Figure 2 shows the current sensitivity in voltage imaging under conventional wide-field illumination. An expanded 532-nm laser beam was utilized to overfill the back opening of the objective and evenly illuminate the object plane. In this experiment, a L5 pyramidal neuron was labeled with a voltage-sensitive dye. A basal dendrite with spines positioned close to

the surface of the slice (to minimize light scattering) was selected under low fluorescent light level. The magnified image of the dendrite was projected to a 80×80 pixels CCD camera for voltage imaging [Fig. 2(a)]. The spine was positioned in the immediate vicinity ($\sim 0.5 \mu\text{m}$) of the center of the field of view where a diffraction-limited uncaging spot from a femtosecond laser could be delivered. During a 50-ms optical recording period [Fig. 2(b)], the subthreshold signal adjusted to mimic a unitary EPSP was evoked by two-photon glutamate uncaging using 720-nm light from a femtosecond-pulsed laser (for experimental details see Ref. 43). A strong depolarizing current pulse delivered from the somatic patch pipette to evoke an AP, which backpropagated into the basal dendrite (bAP), followed the EPSP signal. Figure 2 clearly shows that the sensitivity of voltage imaging was adequate to monitor, quantify, and compare the subthreshold signals from spine heads and the dendritic region at the base of the spine. Previously reported measurements⁴³ were improved here by recording both signals in the same sweep at the frame rate of 5 kHz so that signals can be accurately reconstructed for calibration and comparison.

The success rate of these measurements, however, was relatively low, between 10% and 20%. This is because light scattering from the relatively large parent dendrites was found to contaminate the signal from the small spine head in experiments in which the dendrite is deeper than 15 to 20 μm below the surface of the brain slice. Another constraint was the photodynamic damage that limits the intensity of the excitation light and, hence, the S/N that can be attained. With these technical limitations, it would be difficult or impossible to study directly more complex phenomena in electrical signaling in individual spines because these studies would require repeated measurements under different conditions. Thus, further improvement in voltage imaging was critical. We took advantage of a holographic illumination technique as recently developed and introduced to neurobiology.^{45–49,55,59–62}

To reduce photodynamic damage and scattered light, we replaced the wide-field illumination of the entire dendritic branch with a patterned illumination based on CGH that produced several diffraction-limited spots positioned on the regions

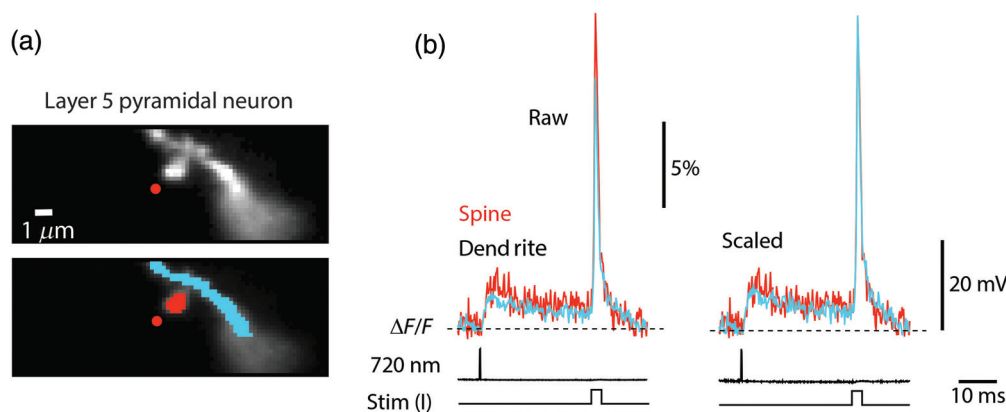


Fig. 2 Voltage-sensitive dye recordings under wide-field illumination in epifluorescence microscopy mode. (a) Upper panel: fluorescence image of a basal dendrite branch with one spine in focus with 100 \times objective. The red dot indicates the position of a stationary spot for two-photon uncaging. Lower panel: selection of pixels for spatial averaging of spine signal (red) and parent dendrite signals (blue). (b) Optical signals related to uncaging evoked EPSP and a subsequent bAP initiated by a depolarizing current pulse and used as a calibration standard. In the right panel, AP signals are scaled to the same height to correct for the difference in sensitivity in recordings from different locations. This is necessary for calibration of optical signals in terms of membrane potential.

of interest (Fig. 3). In a set of initial experiments, we used wide-field fluorescence images of dendritic branches with spines [Fig. 3(a)] to select the pattern of illumination [Fig. 3(b)] with excitation spots generated using a graphic interface for CGH.^{55,63} In this way, only several diffraction-limited spots at selected regions excited the voltage-sensitive dye. The result of patterned illumination is shown in Fig. 3(c). In addition to spatial shaping of illumination, CGH also enables modulation of the relative intensity of individual excitation spots to achieve optimal recording conditions.⁵³ In the three examples shown in Fig. 3, dendritic regions at the base of the spine were not illuminated while the locations away from dendritic spines were illuminated with lower intensities. In every experiment, this resulted in an increase in the resting fluorescence intensity ratio between spine and parent dendrite. Figure 3(d) shows that, in different experiments, the ratio increased by a factor of 2 to 14 depending on the applied pattern of illumination. In this way, contamination of spine signals by light scattered from parent dendrites is minimized or practically eliminated. Therefore, this unique illumination scheme based on CGH allows for recording from spines attached to thick and deeper dendrites. Previously, it was not possible to probe these spines for electrical signals by any method because of high intensity of scattered light. We conclude that the control of the spatial distribution of illumination sites and the adjustments of relative intensities between excitation spots should achieve an optimal compromise between the S/N and photodynamic damage in recordings from spine heads and parent dendrites.

To test this prediction, in the next series of experiments, we determined the sensitivity of recording and the extent of photodynamic damage under patterned illumination by monitoring evoked subthreshold and bAP signals. In the experiment

shown in Fig. 4, the patterned illumination was generated so that a spine head and six locations on the dendrite were selectively illuminated, as indicated by the distribution of green circles on the wide-field fluorescence image of the dendritic region in the recording position [Fig. 4(a)]. Because of this selective illumination pattern, the dendritic area at the base of the spine was not illuminated. This minimizes the contamination of the spine signal by the scattered light from the parent dendrite. Additionally, the relative intensity of the illumination spots was adjusted so that the illuminated dendritic regions received only 50% of the illumination density delivered to the spine. In addition to reducing the light-scattering effect, the graded illumination minimized the photodynamic damage. At the same time, the loss in the S/N due to lower fluorescence intensity from the dendrite was compensated for by the larger dendritic membrane area from which the light was collected. The optical recording was carried out at the frame rate of 5 kHz during a subthreshold membrane potential transient and a subsequent AP. Both signals were evoked by transmembrane depolarizing current steps delivered from the somatic patch pipette. In this recording, the dendritic signal is the temporal average of nine trials and a spatial average of 125 individual pixels from the remote dendritic area indicated by the blue ellipse in Fig. 4(a) while the spine signal is the spatial average of only 22 pixels. It is clear that the sensitivity was adequate for monitoring both subthreshold and suprathreshold responses from the spine and dendrite. In basal dendrites of L5 pyramidal neurons, the optical signal can be calibrated in terms of membrane potential using the size of the spike as a calibration standard because bAP amplitude is known from electrical measurements.⁵⁷ In the experiment shown in Fig. 4, the bAP optical signal corresponds to a spike of ~ 70 mV. Thus, the

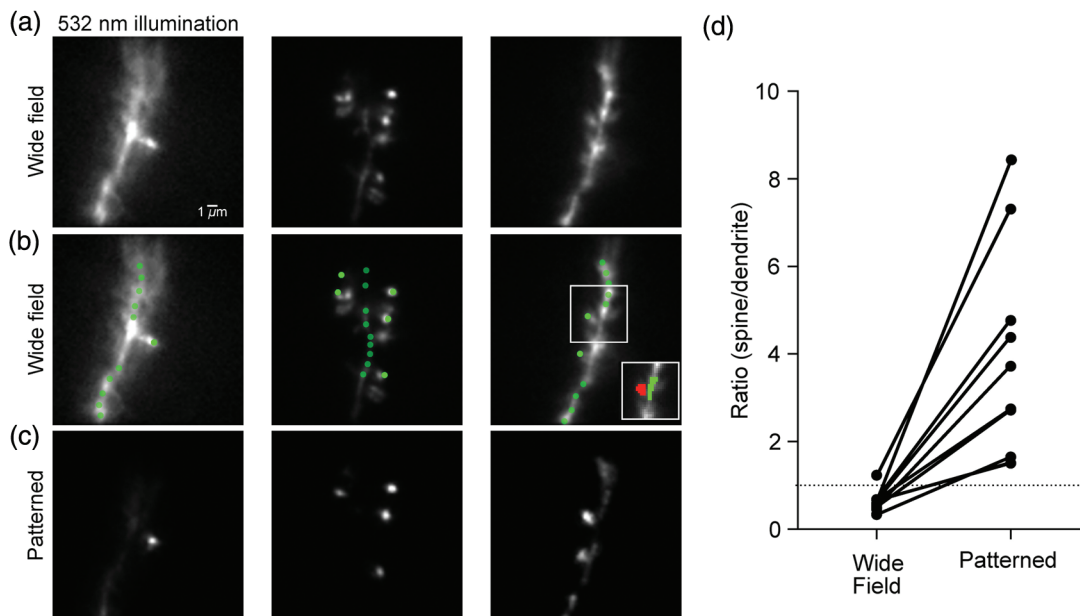


Fig. 3 Contrast improvement with intensity gradient holographic illumination. (a) Fluorescence images of small sections of basal dendrites from three L5 pyramidal neurons under wide-field illumination obtained by a large homogeneous CGH pattern covering the whole field of view. Scale bar: 1 μm . (b) Scheme of the multispot CGH illumination patterns superimposed on the wide-field fluorescence image. (c) VSD fluorescence under CGH-patterned illumination. (d) Increase in contrast expressed as the fluorescence intensity ratio between spines and parent dendrites as determined in nine different preparations. The dramatic increase in the intensity ratio by a factor of 2 to 14 corresponds to an equivalent decrease in the contamination of the spine signal by scattered light from the parent dendrite.

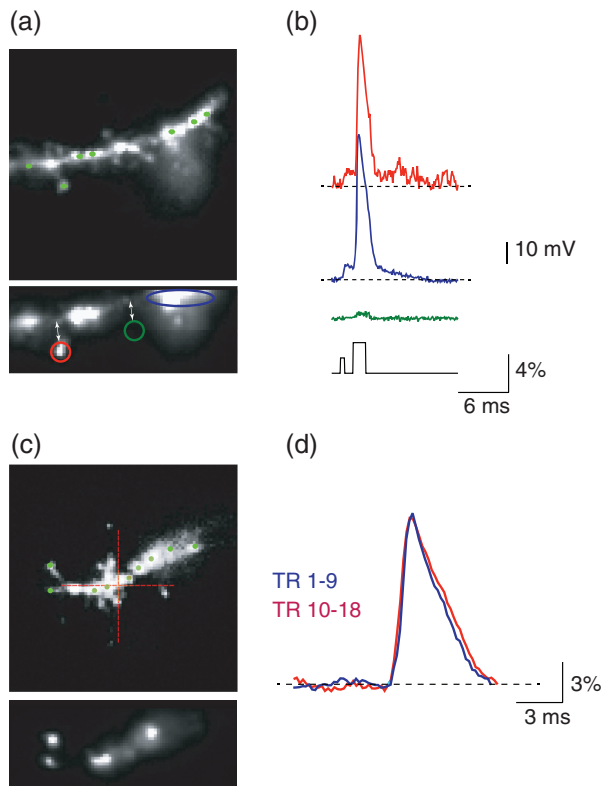


Fig. 4 Sensitivity of optical recording using digital holography-patterned illumination. (a) Upper panel: fluorescence image of a section of basal dendrite under wide-field illumination used to define illumination pattern. Lower panel corresponds to central subsection of the camera chip used for data acquisition at a frame rate of 5 kHz. It shows the same dendritic section under patterned illumination. (b) Optical signals corresponding to a subthreshold and suprathreshold (bAP) response from a spine head (red) and from a remote dendritic region (blue). The green trace is recorded from a region without spine (green circle) at the same distance from the parent dendrite as the recorded spine head. The absence of signal indicates significant reduction of light scattering with holographic patterned illumination. (c) Upper panel: fluorescence image of another section of basal dendrite under wide-field illumination used to define illumination pattern. Lower panel shows the same dendritic section under patterned illumination. (d) Optical signals from the entire structure under holographic illumination. The signal from the first nine trials used for temporal averaging (blue) is very nearly identical to the average signal from the subsequent nine trials. The result indicates absence of photodynamic damage under holographic illumination at the excitation light intensity that produces unprecedented sensitivity (S/N in recording bAP of ~ 30 determined as signal amplitude divided by the second largest peak-to-peak noise amplitude).

data show that, with CGH, it was possible to resolve local subthreshold signals from individual spines that are of the order of 5 mV. The sensitivity can be further improved by additional temporal averaging and/or by increasing the excitation light intensity. We did not detect any photodynamic damage with holographic illumination at the light intensity that provided adequate sensitivity in terms of the S/N . Figures 4(c) and 4(d) show the absence of photodynamic damage in measurements that included 18 trials. The spike waveform, which is a very sensitive indicator of the state of voltage sensitive channels and overall membrane excitability, remained practically identical during the first and the second series of nine recordings. In this study, we did not systematically explore the limits in

excitation light intensity set by photodynamic damage because the relationship between these two variables is complex, requiring extensive analysis.

In the next series of experiments, we combined the two patterned illumination systems at 532 and 405 nm to achieve a configuration allowing, for the first time, simultaneous multisite glutamate uncaging and voltage imaging. We carried out these initial experiments using a one-photon photolysis of DMI-glutamate to establish the feasibility of using two independently controlled SLM systems to realize simultaneous voltage imaging and scanless multiple site glutamate uncaging. In the experiment shown in Fig. 5(a), illumination spots for voltage imaging (green) were generated by one SLM system. Additionally, two diffraction limited spots for glutamate uncaging generated by a separate SLM using 405-nm laser light (blue) were positioned in close proximity to two spine heads.⁴⁷ In this arrangement, it was possible to record subthreshold optical signals from a remote spine and parent dendrite in response to glutamate uncaging onto either one or two spines simultaneously [Figs. 5(c)–5(f)]. Uncaging and recording from the same spine was not possible because of the inadequate spatial resolution of one-photon photolysis (see Sec. 4). Following subthreshold responses, an AP was evoked by a depolarizing current delivered from the somatic patch electrode. The bAP signal was used to normalize the sensitivity of recording from different structures. The results demonstrated the functionality of the system for simultaneous uncaging and voltage imaging with single spine resolution using CGH.

4 Discussion

In this study, we replaced the standard wide-field illumination in voltage imaging with a two-wavelength patterned illumination system based on CGH, with the goal of improving investigation of individual dendritic spines by voltage imaging and glutamate uncaging. CGH is a technique based on phase modulation of coherent light initially developed for the generation of “optical tweezers.” This powerful technique has been considered a revolution in light manipulation.⁴ Lately, the technique acquired a major role in neurobiology, where it has been applied to carry out both single- and two-photon uncaging,^{46–49,55} optogenetic stimulation,^{62,64–67} and functional imaging.^{45,59–61} Here, we demonstrate a dual-color CGH illumination system especially designed to perform functional recording from dendritic spines, where a first optical path is used to generate multisite intensity graded patterns, allowing localization and intensities adjustment of the illumination of dendrites and spine heads, and the second path permits a simultaneous multisite uncaging. Voltage imaging has been systematically developed from the early days of pioneering studies^{5,11,14,18,68,69} to the level where it is now possible to monitor electrical signals from individual dendritic spines in brain slices.^{20,42,43,70} Nevertheless, the limitations in voltage imaging caused by photodynamic damage and by light scattering in the brain tissue still prevent the study of electrical phenomena in dendritic spines that are too complex to be investigated by simple experimental protocols. We carried out experiments to demonstrate the possibility of using CGH illumination to perform voltage imaging from multiple spines and the parent dendrite. Intensity-graded illumination patterns, defined based on fluorescence images, were shaped in a way to practically eliminate contamination of optical signals by the scattered light from the parent dendrite [Figs. 4(a) and 4(b)], increasing the effective spatial resolution of functional

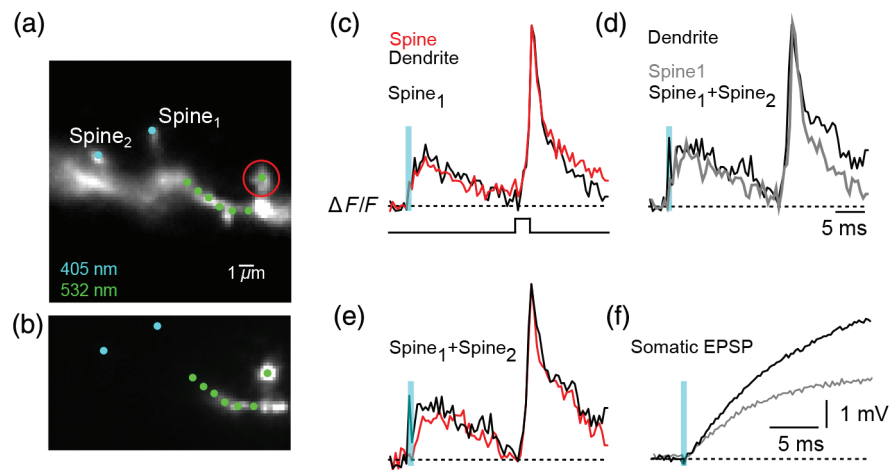


Fig. 5 Simultaneous voltage imaging and scanless glutamate uncaging from individual spines using two independently controlled and synchronized CGH patterns of illumination. (a) Fluorescence image of a section of basal dendrite under wide-field illumination used to generate illumination pattern for voltage imaging (green) and glutamate uncaging (blue). (b) The same dendritic section under patterned illumination. (c) Optical signals corresponding to a subthreshold signal evoked by glutamate uncaging onto one spine and suprathreshold (bAP) response evoked by depolarizing current pulse. Signals from spine head (red) and from parent dendrite (black) are shown. (d) Comparison of subthreshold signals from the dendritic region at the base of the spine evoked by uncaging glutamate onto one spine and two spines simultaneously. (e) Signals from spine head (red) and parent dendrite (black) evoked by simultaneous uncaging of glutamate onto two spines. (f) Patch electrode somatic recordings of the subthreshold responses related to glutamate uncaging onto one and two spines.

recording. The results also suggest that the localization of the illumination exclusively on the regions of interest (spine heads and small sections on parent dendrites) can significantly reduce photodynamic damage [Figs. 4(c) and 4(d)]. Finally, we showed that voltage imaging with CGH at 532-nm excitation light could be combined with patterned illumination for a simultaneous multisite glutamate uncaging. Uncaging was implemented with an independently controlled holography system using 405-nm light for one-photon uncaging. Thus, uncaging and recording from the same spine were not possible because of the inadequate spatial resolution of one-photon photolysis. In most cases, the diameter of the illumination spots was enlarged (relative to the diffraction-limited spot) due to light scattering in the brain slice tissue. The large uncaging light spot positioned near the spine would excite the voltage sensitive dye in the spine head membrane. This resulted in an artifact signal that masked the real response (not shown). This problem is resolved using photolysis based on two-photon absorption characterized by diffraction-limited spatial resolution, as shown in Fig. 2. Thus, the use of CGH under two-photon excitation would permit better preservation of the pattern of illumination against the effect of tissue scattering⁷¹ and investigation of deeper structures. Additionally, the demonstrated capability of CGH to generate patterns over multiple planes^{47,54} coupled with an extended-depth-of-field detection^{60,72} could allow simultaneous volumetric photoactivation and detection of multiple spines. These developments will facilitate further imaging studies of how specific combinations of different transmitter receptors and voltage-sensitive ion channels in different classes of spines act in concert to shape the integration of chemical input signals at the site of origin.⁷³

Disclosures

No conflicts of interest, financial or otherwise, are declared by the authors.

Acknowledgments

We thank Christophe Tourain and Eirini Papagiakoumou for their help in designing and building up the holographic system. VE thanks the Agence Nationale de la Recherche (ANR-WaveFrontImag, ANR-10-INBS-04-01, France-BioImaging Infrastructure Network). We are grateful to Leslie M. Loew (Centre for Cell Analysis and Modelling, UConn Health Centre, Farmington, Connecticut) for kindly providing dyes. This work was supported in part by the National Institutes of Health award (MH106906) and BRAIN Initiative award (1U01NS099691) to DZ.

References

1. G. J. Stuart, H. U. Dodt, and B. Sakmann, "Patch-clamp recordings from the soma and dendrites of neurons in brain slices using infrared video microscopy," *Pflugers Arch.* **423**, 511–518 (1993).
2. G. J. Stuart and B. Sakmann, "Active propagation of somatic action potentials into neocortical pyramidal cell dendrites," *Nature* **367**, 69–72 (1994).
3. M. E. Larkum, J. J. Zhu, and B. Sakmann, "Dendritic mechanisms underlying the coupling of the dendritic with the axonal action potential initiation zone of adult rat layer 5 pyramidal neurons," *J. Physiol.* **533**, 447–466 (2001).
4. D. G. Grier, "A revolution in optical manipulation," *Nature* **424**, 810–816 (2003).
5. A. Grinvald, W. N. Ross, and I. Farber, "Simultaneous optical measurements of electrical activity from multiple sites on processes of cultured neurons," *Proc. Natl. Acad. Sci. U. S. A.* **78**, 3245–3249 (1981).
6. A. Grinvald and I. C. Farber, "Optical recording of calcium action potentials from growth cones of cultured neurons with a laser microbeam," *Science* **212**, 1164–1167 (1981).
7. T. D. Parsons et al., "Optical recording of the electrical activity of synaptically interacting Aplysia neurons in culture using potentiometric probes," *Biophys. J.* **56**, 213–221 (1989).
8. T. D. Parsons et al., "Long-term optical recording of patterns of electrical activity in ensembles of cultured Aplysia neurons," *J. Neurophysiol.* **66**, 316–333 (1991).

9. S. Rohr and B. M. Salzberg, "Characterization of impulse propagation at the microscopic level across geometrically defined expansions of excitable tissue: multiple site optical recording of transmembrane voltage (MSORTV) in patterned growth heart cell cultures," *J. Gen. Physiol.* **104**, 287–309 (1994).
10. W. N. Ross and V. Krauthamer, "Optical measurements of potential changes in axons and processes of neurons of a barnacle ganglion," *J. Neurosci.* **4**, 659–672 (1984).
11. H. V. Davila et al., "Changes in ANS and TNS fluorescence in giant axons from *Loligo*," *J. Membr. Biol.* **15**, 29–46 (1974).
12. L. B. Cohen et al., "Changes in axon fluorescence during activity: molecular probes of membrane potential," *J. Membr. Biol.* **19**, 1–36 (1974).
13. B. Salzberg, "Optical signals from giant axon following perfusion or superfusion with potentiometric probes," *Biol. Bull.* **155**, 463–464 (1978).
14. R. K. Gupta et al., "Improvements in optical methods for measuring rapid changes in membrane potential," *J. Membr. Biol.* **58**, 123–137 (1981).
15. A. Obaid, H. Shimizu, and B. Salzberg, "Intracellular staining with potentiometric dyes: optical signals from identified leech neurons and their processes," *Biol. Bull.* **163**, 388 (1982).
16. A. Grinvald et al., "Optical recording of synaptic potentials from processes of single neurons using intracellular potentiometric dyes," *Biophys. J.* **51**, 643–651 (1987).
17. A. Waggoner and A. Grinvald, "Mechanisms of rapid optical changes of potential sensitive dyes," *Ann. N.Y. Acad. Sci.* **303**, 217–242 (1977).
18. A. Grinvald et al., "Improved fluorescent probes for the measurement of rapid changes in membrane potential," *Biophys. J.* **39**, 301–308 (1982).
19. L. B. Cohen and S. Leshner, "Optical monitoring of membrane potential: methods of multisite optical measurement," *Soc. Gen. Physiol. Ser.* **40**, 71–99 (1986).
20. K. Holthoff, D. Zecevic, and A. Konnerth, "Rapid time course of action potentials in spines and remote dendrites of mouse visual cortex neurons," *J. Physiol.* **588**, 1085–1096 (2010).
21. M. Djurusic et al., "Voltage imaging from dendrites of mitral cells: EPSP attenuation and spike trigger zones," *J. Neurosci.* **24**, 6703–6714 (2004).
22. M. Djurusic et al., "Functional structure of the mitral cell dendritic tuft in the rat olfactory bulb," *J. Neurosci.* **28**, 4057–4068 (2008).
23. W.-L. Zhou et al., "Dynamics of action potential backpropagation in basal dendrites of prefrontal cortical pyramidal neurons," *Eur. J. Neurosci.* **27**, 923–936 (2008).
24. C. D. Acker and S. D. Antic, "Quantitative assessment of the distributions of membrane conductances involved in action potential backpropagation along basal dendrites," *J. Neurophysiol.* **101**, 1524–1541 (2009).
25. R. Yuste and W. Denk, "Dendritic spines as basic functional units of neuronal integration," *Nature* **375**, 682–684 (1995).
26. B. L. Sabatini, T. G. Oertner, and K. Svoboda, "The life cycle of Ca²⁺ ions in dendritic spines," *Neuron* **33**, 439–452 (2002).
27. J. Noguchi et al., "Spine-neck geometry determines NMDA receptor-dependent Ca²⁺ signaling in dendrites," *Neuron* **46**, 609–622 (2005).
28. W. Rall, "Cellular mechanisms subserving changes in neuronal activity," in *The Theoretical Foundation of Dendritic Function*, MIT Press, London, England (1974).
29. C. Koch and A. Zador, "The function of dendritic spines: devices subserving biochemical rather than electrical compartmentalization," *J. Neurosci.* **13**, 413–422 (1993).
30. C. Sala and M. Segal, "Dendritic spines: the locus of structural and functional plasticity," *Physiol. Rev.* **94**, 141–188 (2014).
31. I. Segev and W. Rall, "Excitable dendrites and spines: earlier theoretical insights elucidate recent direct observations," *Trends Neurosci.* **21**, 453–460 (1998).
32. J. Jack, D. Noble, and R. Tsien, *Electric Current Flow in Excitable Cells*, Oxford University Press, London (1975).
33. B. L. Bloodgood and B. L. Sabatini, "Neuronal activity regulates diffusion across the neck of dendritic spines," *Science* **310**, 866–869 (2005).
34. R. Araya et al., "The spine neck filters membrane potentials," *Proc. Natl. Acad. Sci. U. S. A.* **103**, 17961–17966 (2006).
35. R. Araya, K. B. Eiselthaler, and R. Yuste, "Dendritic spines linearize the summation of excitatory potentials," *Proc. Natl. Acad. Sci. U. S. A.* **103**, 18799–18804 (2006).
36. M. T. Harnett et al., "Synaptic amplification by dendritic spines enhances input cooperativity," *Nature* **491**, 599–602 (2012).
37. A. T. Gullledge, N. T. Carnevale, and G. J. Stuart, "Electrical advantages of dendritic spines," *PLoS One* **7**, e36007 (2012).
38. C. D. Acker, E. Hoyos, and L. M. Loew, "EPSPs measured in proximal dendritic spines of cortical pyramidal neurons," *Neuro* **3**, 1–13 (2016).
39. K. Jayant et al., "Targeted intracellular voltage recordings from dendritic spines using quantum-dot-coated nanopipettes," *Nat. Nanotechnol.* **12**(4), 335–342 (2017).
40. K. Svoboda, D. W. Tank, and W. Denk, "Direct measurement of coupling between dendritic spines and shafts," *Science* **272**, 716–719 (1996).
41. J. Tønnesen et al., "Spine neck plasticity regulates compartmentalization of synapses," *Nat. Neurosci.* **17**, 678–685 (2014).
42. M. A. Popovic et al., "Cortical dendritic spine heads are not electrically isolated by the spine neck from membrane potential signals in parent dendrites," *Cereb. Cortex* **24**, 385–395 (2014).
43. M. A. Popovic et al., "Electrical behaviour of dendritic spines as revealed by voltage imaging," *Nat. Commun.* **6**, 8436 (2015).
44. A. L. Obaid et al., "Spatiotemporal patterns of activity in an intact mammalian network with single-cell resolution: optical studies of nicotinic activity in an enteric plexus," *J. Neurosci.* **19**, 3073–3093 (1999).
45. A. J. Foust et al., "Computer-generated holography enhances voltage dye fluorescence discrimination in adjacent neuronal structures," *Neurophotonics* **2**, 21007 (2015).
46. F. Anselmi et al., "Three-dimensional imaging and photostimulation by remote-focusing and holographic light patterning," *Proc. Natl. Acad. Sci. U. S. A.* **108**, 19504–19509 (2011).
47. S. Yang et al., "Three-dimensional holographic photostimulation of the dendritic arbor," *J. Neural Eng.* **8**, 46002 (2011).
48. V. Nikolenko, "SLM microscopy: scanless two-photon imaging and photostimulation using spatial light modulators," *Front. Neural Circuits* **2**, 1–14 (2008).
49. V. R. Daria et al., "Arbitrary multisite two-photon excitation in four dimensions," *Appl. Phys. Lett.* **95**, 093701 (2009).
50. M. Dal Maschio et al., "Simultaneous two-photon imaging and photo-stimulation with structured light illumination," *Opt. Express* **18**, 18720–18731 (2010).
51. S. Antic and D. Zecevic, "Optical signals from neurons with internally applied voltage-sensitive dyes," *J. Neurosci.* **15**, 1392–1405 (1995).
52. R. Di Leonardo, F. Ianni, and G. Ruocco, "Computer generation of optimal holograms for optical trap arrays," *Opt. Express* **15**, 1913–1922 (2007).
53. R. Conti et al., "Computer generated holography with intensity-graded patterns," *Front. Cell. Neurosci.* **10**, 236 (2016).
54. O. Hernandez et al., "Three-dimensional spatiotemporal focusing of holographic patterns," *Nat. Commun.* **7**, 11928 (2016).
55. C. Lutz et al., "Holographic photolysis of caged neurotransmitters," *Nat. Methods* **5**, 821–827 (2008).
56. G. Stuart and N. Spruston, "Determinants of voltage attenuation in neocortical pyramidal neuron dendrites," *J. Neurosci.* **18**, 3501–3510 (1998).
57. T. Nevian et al., "Properties of basal dendrites of layer 5 pyramidal neurons: a direct patch-clamp recording study," *Nat. Neurosci.* **10**, 206–214 (2007).
58. L. M. Palmer and G. J. Stuart, "Membrane potential changes in dendritic spines during action potentials and synaptic input," *J. Neurosci.* **29**, 6897–6903 (2009).
59. S. Bovetti et al., "Simultaneous high-speed imaging and optogenetic inhibition in the intact mouse brain," *Sci. Rep.* **7**, 40041 (2017).
60. S. Quirin et al., "Simultaneous imaging of neural activity in three dimensions," *Front. Neural Circuits* **8**, 29 (2014).
61. W. Yang et al., "Simultaneous multi-plane imaging of neural circuits," *Neuron* **89**, 269–284 (2016).
62. I. Reutsky-Gefen et al., "Holographic optogenetic stimulation of patterned neuronal activity for vision restoration," *Nat. Commun.* **4**, 1509 (2013).
63. E. Papagiakoumou et al., "Scanless two-photon excitation of channelrhodopsin-2," *Nat. Methods* **7**, 848–854 (2010).

64. E. Chaigneau et al., "Two-photon holographic stimulation of ReaChR," *Front. Cell. Neurosci.* **10**, 234 (2016).
65. A. M. Packer et al., "Simultaneous all-optical manipulation and recording of neural circuit activity with cellular resolution in vivo," *Nat. Methods* **12**, 140–146 (2015).
66. E. Ronzitti et al., "Sub-millisecond optogenetic control of neuronal firing by two-photon holographic photoactivation of Chronos," *BioRxiv* 062182 (2016).
67. A. Bègue et al., "Two-photon excitation in scattering media by spatiotemporally shaped beams and their application in optogenetic stimulation," *Biomed. Opt. Express* **4**, 2869–2879 (2013).
68. H. V. Davila et al., "A large change in axon fluorescence that provides a promising method for measuring membrane potential," *Nature* **241**, 159–160 (1973).
69. B. M. Salzberg et al., "Optical recording of neuronal activity in an invertebrate central nervous system: simultaneous monitoring of several neurons," *J. Neurophysiol.* **40**, 1281–1291 (1977).
70. M. Popovic et al., "Imaging submillisecond membrane potential changes from individual regions of single axons, dendrites and spines," in *Membrane Potential Imaging in the Nervous System and Heart*, pp. 57–101, Springer, Heidelberg, New York, London (2015).
71. E. Papagiakoumou et al., "Functional patterned multiphoton excitation deep inside scattering tissue," *Nat. Photonics* **7**, 274–278 (2013).
72. S. Quirin, D. S. Peterka, and R. Yuste, "Instantaneous three-dimensional sensing using spatial light modulator illumination with extended depth of field imaging," *Opt. Express* **21**, 16007–16021 (2013).
73. O. A. Shipton et al., "Left-right dissociation of hippocampal memory processes in mice," *Proc. Natl. Acad. Sci. U. S. A.* **111**, 15238–15243 (2014).

Dimitrii Tanese is a postdoctoral researcher at the Wavefront Engineering Microscopy Group (Neurophotonics Laboratory, Paris). His research focuses on the development of optical methods for functional imaging and neuronal photoactivation based on shaped illumination. Previously, he obtained his PhD (2010 to 2013) from the University Pierre et Marie Curie in Paris, working on nonlinear optics in semiconductor microcavities at the CNRS Laboratory of Photonique and Nanostructures, Marcoussis, France.

Ju-Yun Weng is a postdoctoral associate in Dr. Zecevic's Lab at Yale University School of Medicine. He obtained his PhD in neuroscience at the National Yang-Ming University in Taiwan. He used electrophysiological and voltage imaging techniques to investigate acid-sensing ion channels and axonal signal integration on hippocampal

GABAergic interneurons. He currently works with Dr. Zecevic on electrical structure of cortical dendritic spines using voltage imaging.

Valeria Zampini is a research engineer at the Wavefront Engineering Microscopy Group (Neurophotonics Lab. Paris). She worked as a postdoc at the École normale supérieure, Paris, France, where she studied synaptic integration in interneurons of the vestibulo-cerebellum. During her PhD and first postdoctoral training, she studied vestibular and cochlear hair cells physiology and Cav1.3 calcium channels responsible for synaptic release in these receptors (University of Pavia, Italy; University of Sheffield, United Kingdom).

Vincent De Sars is a research engineer at the Wavefront Engineering Microscopy Group (Neurophotonics Lab. Paris) specializing in software development and instrumentation. He developed the software Wavefront Designer IV for the generation of holographic phase patterns.

Marco Canepari is an INSERM first-class researcher working in the Laboratoire Interdisciplinaire de Physique in Grenoble. He obtained his PhD at SISSA/ISAS in Trieste and worked in several laboratories as a postdoctoral scientist, including the laboratory of Dejan Zecevic at Yale University School of Medicine.

Balázs Rózsa is the head of the Two-Photon Imaging Center at the Institute of Experimental Medicine Semmelweis University Budapest, Budapest, Hungary.

Valentina Emiliani is the director of the Neurophotonics Laboratory at Paris Descartes University. She obtained her PhD in physics at the University 'La Sapienza' Rome. As a postdoc, she investigated carrier transport in quantum wires (Max Born Institut, Berlin) and light propagation in disordered structures (LENS, Florence) by SNOM and cell mechanotransduction by optical tweezers (Institute Jacques Monod, Paris). In 2005, she formed wavefront engineering microscopy, pioneering the use of wavefront shaping for neuroscience.

Dejan Zecevic is a senior research scientist at Yale University School of Medicine. He received his PhD in biophysics from the University of Belgrade, Serbia, and was trained in the laboratory of Dr. Lawrence Cohen, a pioneer in voltage imaging. His work on the electrical and functional structure of individual neurons utilizes intracellular voltage-sensitive dye imaging technique, a unique and a cutting-edge technology for monitoring membrane potential signals in axons, dendrites, and dendritic spines.